Receding-Horizon Estimation and Control of Ball Mill Circuits

Renato Lepore[1], Alain Vande Wouwer[1], Marcel Remy[1], and Philippe Bogaerts[2]

[1] Service d'Automatique, Faculté Polytechnique de Mons, Boulevard Dolez 31, B-7000 Mons, Belgium
{renato.lepore,alain.vandewouwer,marcel.remy}@fpms.ac.be
[2] Chimie Générale et Biosystèmes, Université Libre de Bruxelles, Avenue F.D. Roosevelt 50, B-1050 Bruxelles, Belgium
philippe.bogaerts@ulb.ac.be

Summary. This paper focuses on the design of a nonlinear model predictive control (NMPC) scheme for a cement grinding circuit, i.e., a ball mill in closed loop with an air classifier. The multivariable controller uses two mass fractions as controlled variables, and the input flow rate and the classifier selectivity as manipulated variables. As the particle size distribution inside the mill is not directly measurable, a receding-horizon observer is designed, using measurements at the mill exit only. The performance of the control scheme in the face of measurement errors and plant-model mismatches is investigated in simulation.

1 Introduction

In cement manufacturing, the grinding process transforms the input material (usually clinker) into a very fine powder (the final product). This process consists of a ball mill in closed loop with an air classifier, where the feed flow rate and the classifier selectivity are used as manipulated variables. The quality indicator used in common practice, which is related to the cement fineness, is the powder specific area or Blaine measurement. Alternative quality indicators can however be defined in terms of the particle size distribution, as further discussed in this study.

Cement grinding circuits can be regulated using standard linear or more advanced nonlinear control schemes [4, 9, 12]. However, most of the control studies reported in the literature consider mass variables only, i.e., mass hold-up of the mill and mass flow rates, whereas control of the product quality requires the consideration of the particle size distribution (or at least, of some related variables). In this connection, a quality control strategy should allow to act on the particle size distribution, as well as to face rapid modification in customer demand (i.e. changes in the cement grade or quality). Hence, efficient setpoint changes have to be achieved despite the process nonlinearities and operating limitations. Such a control strategy appears as an appealing (but challenging) alternative to expensive storage policies.

R. Findeisen et al. (Eds.): Assessment and Future Directions, LNCIS 358, pp. 485–493, 2007.
springerlink.com

In this study, a control scheme is proposed that takes these objectives and constraints into account. The following ingredients are involved in the control design:

- A nonlinear population model describes the dynamic evolution of the mass fractions in three size intervals.
- The mass fractions at the mill outlet and at the product outlet (i.e. the air classifier outlet) can easily be measured in practice using classical sieving techniques. In addition, they can be used, as an interesting alternative to Blaine measurements, to assess the cement quality and performance of the mill.
- A model-based predictive controller is designed in order to achieve quality control and setpoint changes. This control scheme accounts for actuator saturation (in magnitude and rate of change) and for operating and safety constraints, such as mill plugging and temperature increase.
- To reconstruct on-line the particle size distribution (in three size intervals), a receding-horizon observer is designed, which uses measurements available at the mill exit only. This software sensor takes the measurement errors into account and determines the most-likely initial conditions of the prediction horizon.

In previous works [6, 7], the authors have reported on the design of the multivariable controller and of the receding-horizon observer. Here, the main purpose is to study the performance of the combined scheme (i.e. controller + software sensor) in the face of measurement noise and parametric uncertainties. In addition, a DMC-like correction scheme is proposed, which significantly improves the performance of the control strategy in the case of plant-model mismatches. A simulation case study, corresponding to a typical setpoint change, is used to highlight the advantages and limitations of the proposed strategy.

This paper is organized as follows. Section 2 briefly describes the process and the nonlinear model. In Section 3, the control objectives are discussed, the NMPC strategy is introduced, and the software sensor is presented. The combined scheme is evaluated in Section 4 and conclusions are drawn in Section 5.

2 Process Description and Modelling

A typical cement grinding circuit is represented in Figure 1, which consists of a single-compartment ball mill in closed loop with an air classifier. The raw material flow q_C is fed to the rotating mill where tumbling balls break the material particles by fracture and attrition. At the other end, the mill flow q_M is lifted by a bucket elevator into the classifier where it is separated into two parts: the product flow q_P (fine particles) and the rejected flow q_R (coarse particles). The selectivity of the classifier, i.e. the separation curve, influences the product quality. This selectivity can be modified by positioning registers Reg acting on the upward air flow. The material flow q_R is recirculated to the mill inlet and the sum of q_C and q_R is the total flow entering the mill, denoted q_F.

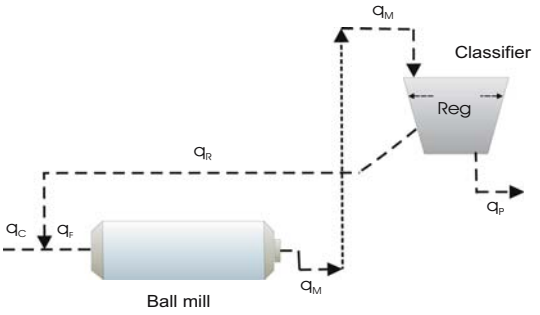

Fig. 1. Closed-loop grinding circuit

A simple population model [5, 6, 7] is used to describe the dynamic evolution of the particle size distribution in three (relatively large) size intervals. This model describes material transportation and breakage inside the ball mill, as well as material separation in the air classifier. This model consists of a set of Partial Differential Equations (PDEs), supplemented by Initial Conditions (ICs) and Boundary Conditions (BCs):

$$\frac{d\mathbf{X}}{dt} = \mathbf{f}_{PDE}\left(\mathbf{X}, \frac{\partial \mathbf{X}}{\partial z}, \frac{\partial^2 \mathbf{X}}{\partial z^2}; \boldsymbol{\theta}_f, \boldsymbol{\theta}_t\right) \tag{1a}$$

$$\mathbf{X}(t_0, z) = \mathbf{X}_0(z), \qquad 0 \le z \le L \tag{1b}$$

$$\mathbf{0} = \mathbf{f}_{BC}\left(\mathbf{X}, \frac{\partial \mathbf{X}}{\partial z}, \mathbf{u}; \boldsymbol{\theta}_t, \boldsymbol{\theta}_{cl}\right), \qquad z = 0, \forall t \tag{1c}$$

$$\mathbf{0} = \frac{\partial \mathbf{X}}{\partial z}, \qquad z = L, \forall t \tag{1d}$$

where the state vector $\mathbf{X}(t, z)$ has 3 components, the k^{th} component being the mass per unit of length (e.g., in tons per meter) in size interval k, at time t and at location z along the mill (L is the mill length). $\mathbf{X}_0(z)$ is the initial-value spatial profile. The input $\mathbf{u}$ has 2 components, q_C and Reg. The parameters $\boldsymbol{\theta}_f$, $\boldsymbol{\theta}_t$ and $\boldsymbol{\theta}_{cl}$ are related to the description of the fragmentation, transportation and classification mechanisms, respectively.

This PDE system is solved numerically using a method of lines [13] strategy. The spatial derivatives are replaced by finite difference approximations, and the resulting system of differential algebraic equations is integrated in time using a readily available solver.

Partitioning the size continuum into three size intervals allows the problem dimension to be reduced as compared to a more detailed description of the particle size distribution (in classical modelling studies 20-30 intervals are considered). Moreover, this specific partition can be directly related to the control objectives, as explained in the next section. In this study, the interval limits (i.e., the upper bounds of the mid-size and small-size intervals) are chosen as 100 and 30 μm.

3 Control Strategy

3.1 Control Objectives and NMPC Scheme

The feed flow rate and the classifier selectivity can be used as manipulated variables. Two mass fractions are used as controlled variables. The first one, denoted w_P^3, corresponds to the fine particles in the product flow. Experimental studies [10] demonstrate that this variable is highly correlated with the compressive strength of the cement, if the upper size of interval 3 is chosen around 30 μm. The second one, denoted w_M^2, corresponds to the mid-size particles in the mill outflow, which can be directly related to the grinding efficiency of the mill (too fine particles correspond to overgrinding whereas too coarse particles correspond to undergrinding).

The use of these several variables is illustrated by the steady-state diagram $w_M^2 = f(q_P, w_P^3)$ of Figure 2, where the curve $\overline{ABC}$ represents all the operating points with $w_P^3 = 0.86$. Clearly, point B corresponds to a maximum product flow rate and, as demonstrated in [3], the arcs $\overline{AB}$ and $\overline{BC}$ correspond to stable and unstable process behaviours, respectively. By setting, for example, $w_M^2 = 0.35$ on arc $\overline{AB}$, a single operating point (point 1) is defined. This corresponds to producing cement of a given fineness ($w_P^3 = 0.86$) at near maximum product flow rate in the stable region. A significant advantage of these controlled variables is that the measurement of mass fractions is simple and inexpensive. A classical sieving technique is used instead of sophisticated (and costly) laser technology.

The design of the NMPC scheme [1, 8] is based on a nonlinear optimization problem, which has to be solved at each sampling time $t_k = kT_s$ (where T_s is the sampling period). More specifically, a cost function measuring the deviation of the controlled variables from the setpoint over the prediction horizon has to be minimized. Denoting $\mathbf{y} = [w_P^3 \; w_M^2]^T$ the controlled variable, the optimization problem is stated as follows:

$$\min_{\{\mathbf{u}_i\}_0^{Nu-1}} \sum_{i=1}^{Np} \left\{\mathbf{y}^s - \hat{\mathbf{y}}(t_{k+i})\right\}^T \mathbf{Q}_i \left\{\mathbf{y}^s - \hat{\mathbf{y}}(t_{k+i})\right\} \tag{2}$$

where Nu and Np are the control and prediction horizon lengths, respectively (number of sampling periods with $Nu < Np$). $\{\mathbf{u}_i\}_0^{Nu-1}$ is the sequence of control moves with $\mathbf{u}_i = \mathbf{u}_{Nu-1}$ for $i \geq Nu$ ($\mathbf{u}_i$ is the input applied to the process model from t_{k+i} to t_{k+i+1}). $\hat{\mathbf{y}}(t_{k+i})$ is the output value at time t_{k+i}, as predicted by the model. $\{\mathbf{Q}_i\}_1^{Np}$ are matrices of dimension 2, weighting the coincidence points. $\mathbf{y}^s$ is the reference trajectory (a piecewise constant setpoint in our study).

In addition, the optimization problem is subject to the following constraints:

$$\mathbf{u}^{min} \leq \mathbf{u}_i \leq \mathbf{u}^{max} \tag{3a}$$

$$-\Delta\mathbf{u}^{max} \leq \Delta\mathbf{u}_i \leq +\Delta\mathbf{u}^{max} \tag{3b}$$

$$q_M^{min} \leq q_M \leq q_M^{max} \tag{3c}$$

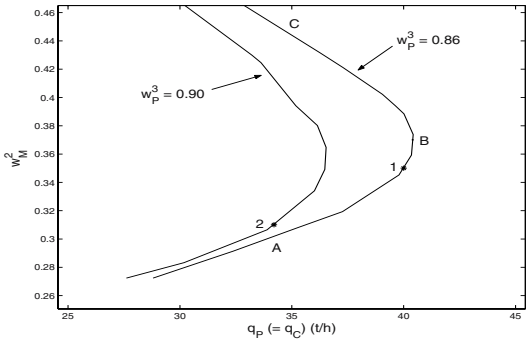

Fig. 2. Steady-state diagram: w_M^2 vs q_P for constant values of w_P^3

On the one hand, equation (3a) represents bound constraints on the manipulated variables, e.g., saturation of the feeding mechanism or in the displacement of the registers, whereas equation (3b) corresponds to limitations of the rate of change of these manipulated variables. On the other hand, equation (3c) expresses constraints on an operating variable, e.g., a lower bound on the mill flow rate to prevent mill emptying and temperature increase, and an upper bound to avoid mill plugging or a drift into the instability region.

3.2 Software Sensor Design

As the particle size distribution inside the mill is not accessible, a receding-horizon observer [1, 11] is designed, based on the nonlinear process model and a few measurements available at the mill exit. The main advantages of this type of software sensors are that a nonlinear model of arbitrary complexity can be used, and the measurement errors can be taken into account rigorously. An estimate of the most-likely initial conditions, noted $\hat{\mathbf{x}}(0|t_k)$, is obtained by solving the following optimization problem:

$$\min_{\mathbf{x}_0} \sum_{i=k-No}^{k} \left\{\mathbf{y}(t_i) - \mathbf{h}_{obs}(\mathbf{x}(t_i), \mathbf{u}(t_i)\right\}^T \boldsymbol{\Sigma}_i^{-1} \left\{\mathbf{y}(t_i) - \mathbf{h}_{obs}(\mathbf{x}(t_i), \mathbf{u}(t_i)\right\}, \quad (4)$$

where $\mathbf{x}_0$ is the initial-condition, No is the prediction horizon length (number of sampling periods $T_o \neq T_s$), $\mathbf{h}_{obs}(.)$ is the output trajectory, $\mathbf{y}(t_i)$ are the measurements affected by a Gaussian white noise with zero mean and covariance matrix $\boldsymbol{\Sigma}_i$.

However, the finite difference schemes used to solve the model equations lead to a relatively large number of state variables which should be estimated. To circumvent this problem, and to keep the optimization problem tractable, the initial condition profile $\mathbf{x}_0(z)$ is approximated by a combination of simple polynomial laws. An approximate representation of the initial spatial profile is sufficient for state estimation and control purposes, as the effect of the initial conditions on

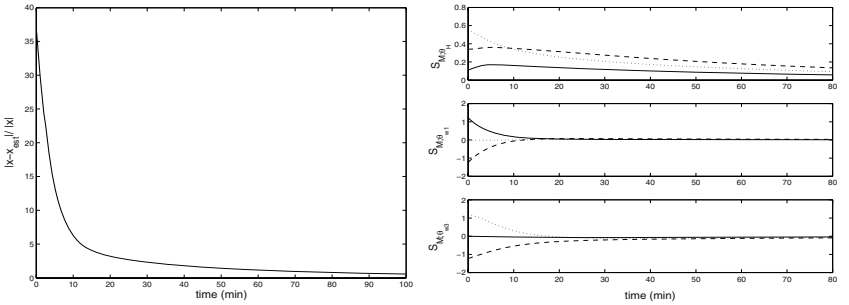

(a) Norm percentage deviation between the real and simulated state

(b) Parametric sensitivity of the mass fractions at the mill outlet; size interval 1:solid, 2:dashed, 3:dotted

Fig. 3. Receding-horizon estimation: evaluating the impact of the initial conditions

the model solution vanishes rapidly as compared to the process time constants. Figure 3(a) shows the norm percentage deviation between the real and simulated state during a typical run. For an initial deviation of about 40 %, the deviation reduces to 5 % in only 10 min.

To build the polynomial approximation, $\mathbf{x}_0(z)$ is expressed in terms of z_r, a scaled spatial coordinate $\left(\frac{z}{L}\right)$, and in terms of the mill material hold-up $H_0(z_r)$ and the mass fractions $w_0^i(z_r)$

$$\mathbf{x}_0(z_r) = H_0(z_r) \left[w_0^1(z_r)\ w_0^2(z_r)\ w_0^3(z_r)\right]^T \tag{5}$$

Simple polynomial laws are then used to represent the several factors of this latter expression. The hold-up is considered uniform $H_0(z_r) = \theta_H$, the mass fraction of coarse particles can be represented by a concave quadratic law $w_0^1(z_r) = 0.3\ z_r(z_r - 2) + \theta_{w1}$, the mass fraction of fine particles can be represented by a convex quadratic law $w_0^3(z_r) = -0.3\, z_r(z_r - 2) + \theta_{w3}$ and $w_0^2(z_r)$ is simply deduced from the two other mass fractions (and is uniform in the present case).

When measurements are available at the mill exit only, it is observed that the relevant information for the determination of θ_{w1} and θ_{w3} vanishes after 10 min. This is apparent in Figure 3(b), which shows the parametric sensitivity of the material mass fractions at the mill outlet. For instance, $S_{M;\theta_H}(t)$ is defined as $\frac{\partial \mathbf{X}}{\partial \theta_H}(L, t)$.

These results justify the use of a simple parameterization of the initial condition profile. In optimization problem (4), a horizon of 20 min with 2 min-sampling intervals is sufficient to ensure convergence and accuracy. On the other hand, the formulation of the state vector using the factorization (5) results in the consideration of simple linear constraints.

The computation time required to solve the optimization problems (2) and (4) would allow the use of shorter sampling intervals, but the measurement procedure (sieving) could be limitative. Here, we have elected to be on the safe side concerning this latter limitation (but shorter sampling intervals would of course improve accuracy and convergence).

4 Numerical Results

In this section, the combined scheme (software sensor + NMPC) is evaluated in simulation, using a typical test run corresponding to a setpoint change. Point 1 in Figure 2 (where $\mathbf{y} = [0.86\ 0.35]^T$) is the initial operating condition, and point 2 (with $\mathbf{y} = [0.90\ 0.31]^T$) represents the target (this point corresponds to a higher product fineness and near maximum product flow rate). The sampling period $T_s = 5$ min and the prediction horizon is 80 min ($Np = 16$). Two manipulated variable moves are used ($Nu = 2$) and the weighting matrix $\mathbf{Q}_i$ is chosen as a constant identity matrix. Amplitude saturations are $q_C^{max} = 60\ \frac{\text{ton}}{\text{hour}}$ and $Reg^{max} = 100$. Limits for the rates of change are $\Delta q_C^{max} = 15 \frac{\text{ton}}{\text{hour}}$ and $\Delta Reg^{max} = 80$. Limits on the mill flow rate are $q_M^{min} = 60\ \frac{\text{ton}}{\text{hour}}$ and $q_M^{max} = 90\ \frac{\text{ton}}{\text{hour}}$. The observer parameters are defined in Section 3.2.

It is first assumed that the process model is accurate and that the measurements are noise free. Figure 4 shows the controlled and the manipulated variables (solid lines). The performance is satisfactory, the controlled variables reach the setpoint after about 20 min and the steady state is obtained after 70 min. Moreover, constraints are active in the first 5 min (first sample), as the maximum register displacement and the maximum rate of change of the input flow rate are required.

The performance of the control scheme is then tested when measurements are subject to a noise with a maximum absolute error of $0.02\ \frac{\text{ton}}{m}$ (around a 5% maximum relative error). The software sensor can efficiently take these stochastic disturbances into account, and the performance of the control scheme remains quite satisfactory.

Finally, the influence of parametric uncertainties (plant-model mismatch due to errors at the identification stage) is investigated. A parametric sensitivity analysis is performed, and Figure 5 shows step responses corresponding to either an accurate model or to a -10% error in the fragmentation rate or the transport velocity. Clearly, fragmentation parameters (which represents material hardness

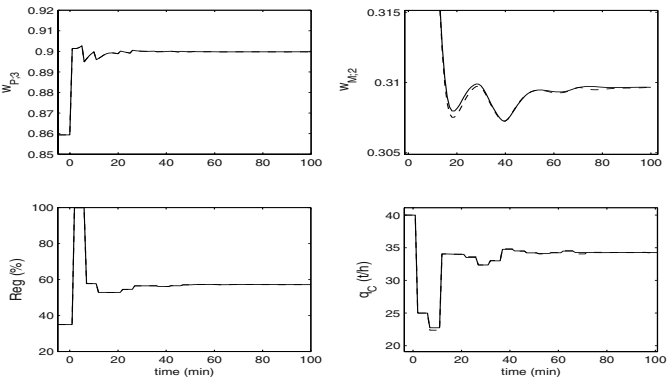

Fig. 4. NMPC and state observer; solid: noise-free measurements, dashed: measurements corrupted by white noise

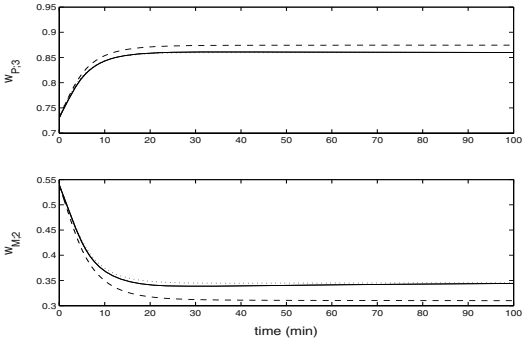

Fig. 5. Parametric sensitivity - Time evolution of the controlled variables; solid: nominal case, dashed: mismatch in the fragmentation rate, dotted: mismatch in the transport velocity

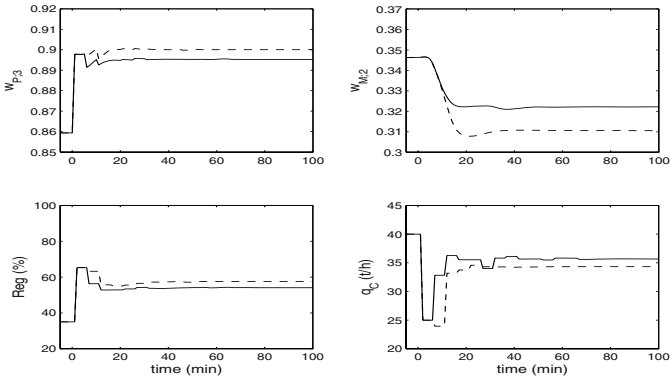

Fig. 6. Plant-model mismatch: solid: without compensation, dotted: with a DMC-like compensation

or grindability) have a larger impact on the model prediction than the material transportation parameters.

The performance of the control scheme is evaluated when a prediction model with erroneous fragmentation rates is used (which is the worst case of plant-model mismatch). Figure 6 shows results corresponding to -5% errors in the fragmentation rates. Clearly, performance deteriorates and a significant steady-state error appears. To alleviate this problem, a DMC-like compensation is proposed, which considers the plant-model mismatch as a constant output disturbance $\hat{\mathbf{d}}_{k+i} = \hat{\mathbf{d}}_k$ over the prediction horizon. An estimate of the disturbance $\hat{\mathbf{d}}_k$ is obtained from the process output $\mathbf{y}_k$ and the observer output, noted $\bar{\mathbf{y}}_k$, as follows:

$$\hat{\mathbf{d}}_k = \mathbf{y}_k - \bar{\mathbf{y}}_k \tag{6}$$

Figure 6 shows that this kind of compensation significantly improves the performance of the control scheme under parametric uncertainties.

5 Conclusion

In this paper, a receding-horizon observer and a receding-horizon controller are designed for a ball mill circuit. The software sensor provides an estimation of the particle size distribution inside the ball mill, based on a nonlinear process model and a few measurements available at the mill exit. The control scheme allows efficient quality control and setpoint changes, even in the face of noisy measurements and significant parametric uncertainties. In addition, a DMC-like compensation of these latter errors improves the performance of the proposed scheme.

References

[1] Allgöwer F., Badgwell T.A., Qin J.S., Rawlings J.B., Wright S.J. (1999) Nonlinear predictive control and moving horizon estimation - an introduction overview. In: Frank P.M. (ed) Advances in Control (Highlights of ECC '99). Springer, London Berlin Heidelberg

[2] Boulvin M. (2000) Contribution à la modélisation dynamique, à la simulation et à la conduite des circuits de broyage à boulets utilisés en cimenterie. PhD Thesis, Faculté Polytechnique de Mons, Mons (Belgium)

[3] Boulvin M., Vande Wouwer A., Lepore R., Renotte C., Remy M. (2003) IEEE transactions on control systems technology 11(5):715–725

[4] Grognard F., Jadot F., Bastin G., Sepulchre R., Wertz V. (2001) IEEE Transactions on Automatic Control 46(4):618–623

[5] Lepore R., Vande Wouwer A., Remy M. (2002) Modeling and predictive control of cement grinding circuits. 15th IFAC World Congress on Automatic Control, Barcelona, Spain

[6] Lepore R., Vande Wouwer A., Remy M. (2003) Nonlinear model predictive control of cement grinding circuits. ADCHEM 2003, Hong-Kong, China

[7] Lepore R., Vande Wouwer A., Remy M., Bogaerts Ph. (2004) State and parameter estimation in cement grinding circuits - practical aspects. DYCOPS 7 2004, Cambridge (MA), U.S.A.

[8] Maciejowski J.M. (2001). Predictive control: with constraints. Prentice Hall

[9] Magni L., Bastin G. and Wertz V. (1999) IEEE transactions on control systems technology 7(4):502–508

[10] Olivier L. (2002) Contribution à la conduite des circuits de broyage à boulets utilisés en cimenterie. MA Thesis. Faculté Polytechnique de Mons, Mons

[11] Rao C.V. (1999) Moving-horizon estimation of constrained and nonlinear systems. PhD Thesis. University of Wisconsin-Madison, Madison

[12] Van Breusegem V., Chen L., Bastin G., Wertz V., Werbrouck V., de Pierpont C. (1996) IEEE Transactions on Industry Applications 32(3):670–677

[13] Vande Wouwer A., Saucez P., Schiesser W.E. (2004) Industrial Engineering and Chemistry Research 43(14):3469–3477